

Journal of Materials Chemistry C

Accepted Manuscript



This is an *Accepted Manuscript*, which has been through the Royal Society of Chemistry peer review process and has been accepted for publication.

Accepted Manuscripts are published online shortly after acceptance, before technical editing, formatting and proof reading. Using this free service, authors can make their results available to the community, in citable form, before we publish the edited article. We will replace this *Accepted Manuscript* with the edited and formatted *Advance Article* as soon as it is available.

You can find more information about *Accepted Manuscripts* in the [Information for Authors](#).

Please note that technical editing may introduce minor changes to the text and/or graphics, which may alter content. The journal's standard [Terms & Conditions](#) and the [Ethical guidelines](#) still apply. In no event shall the Royal Society of Chemistry be held responsible for any errors or omissions in this *Accepted Manuscript* or any consequences arising from the use of any information it contains.

Amorphous Boron-Indium-Zinc-Oxide Active Channel Layers for Thin-Film Transistor Fabrication

Shanmugam Parthiban,[†] and Jang Yeon Kwon^{*,†}

[†]School of Integrated Technology and Yonsei Institute of Convergence and Technology

Yonsei University, Songdo-dong, Incheon, 406-840, Republic of Korea

KEYWORDS Amorphous oxide semiconductor, indium oxide, zinc oxide, thin-film transistor, sputtering,

Highlighting the novelty of the work

Novel amorphous boron-indium-zinc-oxide active channel layer and thin-film transistor fabrication

ABSTRACT: We investigate thin-film transistors (TFT) fabrication, using a novel amorphous boron-indium-zinc-oxide (a-BIZO) thin-film as an active channel layer and radio-frequency sputtering technique. The structural, surface, and optical properties of a-BIZO thin-film were studied. X-ray diffraction (XRD) patterns and high-resolution transmission electron microscopy (HR-TEM) analysis confirmed the amorphous nature of a-BIZO thin-film. Atomic force microscopy revealed a smooth a-BIZO thin-film surface with a uniform and root mean square

roughness of 0.45 nm. The transparency of a-BIZO thin-films was shown to be more than 80% in the wavelength range between 400 and 800 nm, which confirmed a good transparency. The a-BIZO TFT post annealed at 250 °C under the nitrogen atmospheric condition showed a saturation field-effect mobility of 9.6 cm²/V.s, a threshold voltage of 5.3 V, and a subthreshold swing of 0.77 V/dec with an I_{ON}/I_{OFF} current ratio of 2.5×10^7 . The small amount of boron dopant acts as a strong carrier suppressor via the formation of oxygen vacancy in the a-IZO matrix.

INTRODUCTION

Amorphous oxide semiconductors (AOS) are a key material for next generation electronics because of their high mobility, excellent uniform, low temperature deposition and transparency.¹⁻⁶ Most of the research and development has been focused on amorphous Indium-Gallium-Zinc-Oxide (a-IGZO) thin-film transistors (TFT) fabrication as alternatives to amorphous/poly-crystalline silicon (Si) TFT.⁷⁻⁹ However, AOS TFTs require enhanced mobility and stability for next generation displays such as ultra-high-resolution and high-frame-rate-displays.⁷ The a-IZO TFTs can suppress oxygen vacancies (V_o) by adding Ga and reducing the instability of the device.¹⁰ However, for high performance applications, Hf, Zr, Ti, La, Sc, Mg, Ta, W, B, Si, La, and Gd etc., have been incorporated as carrier suppressors instead of Ga.¹⁰⁻²¹ Among the carrier suppressor incorporated in the AOS TFT, the Si incorporation has shown enhanced mobility and stability because of the strong binding dissociation energy of silicon-oxygen (799.6 kJ/mole) thus suppressing carrier concentrations formation via oxygen vacancy.^{11, 13, 20} For enhanced stability, strong bonding dissociation energy between the carrier suppressor and oxide is believed to be a significant property.^{11, 13, 14} However, for enhanced mobility, a clear mechanism has yet to be suggested.

Based on the high Lewis acid strength (L) of dopants, the transparent conducting oxide (TCO) thin-films have been reported with high mobility and visible to near infrared transparency.²³ According to Wen et al., high L dopants polarize the electronic charge away from the oxygen $2p$ valance band more strongly than low L , resulting in screening of the charge and weakening of the activity as a scattering center, hence increasing the mobility.²⁴ The scattering center is a significant parameter to determining mobility if the scattering center is low can be expected high mobility.^{25, 26} The high L elements are suppressed scattering centers that result in high mobility. Based on the high L and strong metal-oxygen bonding dissociation energy, the boron (B) dopant was chosen which retains a unique metal and oxygen bonding dissociation energy.²² Moreover, B retained stable state (3^+), high L (10.7) and strong metal-oxide bonding dissociation energy (~ 808.0 KJ/mole) therefore we believe boron could be a strong carrier suppressor in the AOS thin-films.^{22, 27} In this work, 2.2 mol.% B_2O_3 was chosen in order to avoid the deterioration of TFT performance.²⁸⁻³⁰ Table I summarizes the typical elements that have high L and strong metal-oxygen bonding dissociation energy. Among the elements, B has a high L and strong metal-oxygen bonding strength.

EXPERIMENTAL SECTION

For the a-BIZO, IZO (~ 35 nm) thin-films were deposited on a SiO_2 (100 nm)/Si-p-type substrate using a radio-frequency sputtering technique with the BIZO (22.56/75.4/2.03 mole % of $In_2O_3/ZnO/B_2O_3$) and IZO (25.0/75.0 mole % of In_2O_3/ZnO) (LTS Chemicals, Orangeburg, NY, USA) targets at room temperature. To avoid the sublimation of B_2O_3 powder while preparing the sputtering target the B_2O_3 , In_2O_3 and ZnO were mixed powder was filled with a graphite mold, and then subjected to cold pressing and cold isotactic pressing to perform a green compact. Finally, the graphite mold with the performed green compact was put into a furnace and sintered

at 800 °C for 20 hours. The 4 inch circular target was placed at a distance of 10 cm from the substrate. The sputtering power was fixed at 100 W and the chamber pressure was set at 5 mTorr. The Oxygen/Argon (O_2/Ar) flow ratio varied from 0-9%. The sputtered a-BIZO thin-films were post-annealed at 250 °C for one hour under the nitrogen atmospheric condition. An amorphous structure was confirmed from X-ray diffraction (XRD) (Rigaku-SmartLab), high-resolution transmission electron microscopy (HR-TEM; JSM-ARM200F), and fast Fourier transform (FFT). The composition of a-BIZO thin-films was analyzed using XPS (Thermo Scientific) measurements. The microstructure of the BIZO thin films was investigated using atomic force microscopy (Park-XE-100). The transparency of a-BIZO coated thin-films on Corning glass substrates was analyzed using a double beam spectrophotometer (Cary 5000 UV-Vis-NIR).

To fabricate a-BIZO and IZO TFTs, a 35 nm active layer was deposited on a SiO_2 (100 nm)/Si substrate using RF sputtering at room temperature. The active layer area was patterned using maskless lithography and the liftoff technique. The molybdenum (Mo) (100 nm) source and drain electrode was deposited using DC sputtering at room temperature. The channel width (W) and length (L) of $60 \times 10 \mu m$ was patterned using maskless lithography (DL-1000, Nano system solutions) and the standard liftoff technique. Finally, a sample was subjected to thermal annealing using tubular furnace at 250 °C for 1 hour under the nitrogen (N_2) atmospheric condition. The transfer characteristics of the TFTs were measured at room temperature under a dark condition using a semiconductor parameter analyzer (Keithley SCS 4200).

RESULTS AND DISCUSSION

Figure 1(a) shows the XRD patterns of 100 nm-thick a-BIZO films deposited on Corning glass substrates as a function of O₂/Ar ratio and post annealed at 250 °C under the N₂ atmospheric condition for one hour. Diffraction peaks were not observed in the crystalline phase in the XRD spectra. The spectra indicate that the amorphous nature of the films remained after post annealing at 250 °C for 1 hour. Although these films are nearly three times thicker than the film used for the active channel in the TFTs, it has been reported that thinner films are expected to be even more amorphous in nature.^{31, 32} Fig. 1(b) shows the amorphous characteristics of the a-BIZO thin-film. Additionally, the FFT showed a diffused diffraction pattern that indicates the amorphous nature of the a-BIZO thin-film. The HR-TEM images and FFT pattern clearly indicated that the a-BIZO film grew uniformly and displayed an amorphous phase. Fig. 1(c) shows the surface of an atomic force microscopy image of a-BIZO thin film revealing uniform and smooth morphology, which indicates no crystalline structure. A root mean square roughness of ~ 0.45 nm was observed. The BIZO sputter target and post annealed thin-film were analyzed by XPS measurement, confirmed B/In/Zn composition of 2.4/14.5/17.7 and 3.5/14.3/17.5, respectively.

Figure 2(a) shows the transmittance spectra of a-BIZO (35 nm) thin-film coated on Corning glass substrate with respect to various O₂/Ar ratios. All a-BIZO thin-films were optically transparent and showed an average transmittance exceeding 80% in the wavelength ranging between 400-800 nm. In contrast, the optical band gap (E_g) varied with respect to the O₂/Ar ratio. The values of E_g were obtained by extrapolating the plot of $(\alpha h\nu)^2$ versus $h\nu$ to the intercept (at $\alpha = 0$) for a-BIZO thin-films with respect to the O₂/Ar ratio is shown in Fig. 2(b).³⁴

As the O₂/Ar ratio increased from 1-9%, the values of E_g increased by 3.3-3.6 eV. The variation of E_g increased mainly due to the increased O₂/Ar ratios.³⁵

Figure 3(a) shows the schematic device structure of the bottom gate inverted staggered a-BIZO TFT and fig. 3(b) shows an optical microscopy image of the top-view of the a-BIZO TFT fabrication. The W and L channels were tightly patterned to avoid the fringing effect and over-estimated mobility.³⁶ Figure 4(a) shows the transfer curves of a-BIZO TFT with respect to various O₂/Ar ratios. The 3% O₂/Ar ratio a-IZO (without boron doping) TFT was fabricated with the same deposition condition of 3% O₂/Ar a-BIZO. The 3% O₂/Ar ratio a-IZO was shown to have a more conductive nature, possibly due to the excess carrier concentration. The O₂/Ar was varied from 0 to 9% to determine the optimum condition. The O₂/Ar of 0% and 1% of a-BIZO TFT were shown to have a conductive nature, while 3%, 5%, 7%, and 9 % O₂/Ar TFT were shown to have a good transfer curve. Fig 4 (a) shows the field-effect mobility (μ_{sat}) and turn-on voltage (V_{on}) as function of O₂/Ar, whereas V_{on} shifted to positive direction which can be explained by the reduction of oxygen vacancies in the a-BIZO films.³⁷

The field-effect mobility (μ_{sat}) and subthreshold swing (SS) of the TFTs were estimated in the saturation regime of the transfer curve using the following equations.

$$\mu_{sat} = \left(\frac{\partial \sqrt{I_D}}{\partial V_{GS}} \right)^2 \frac{2L}{W} \frac{1}{C_G}, \quad (1)$$

$$SS = \left(\frac{\partial \log_{10} I_D}{\partial V_{GS}} \right)^{-1}, \quad (2)$$

where I_D is the drain to source current, V_G is the gate to source voltage, V_{th} is the threshold voltage, W and L are the channel width and length, respectively, and C_G is the capacitance per unit area of the gate dielectric. The extracted TFT properties are reported in Table 2. The 3% O₂/Ar ratio a-BIZO TFT exhibited good transfer characteristics at $V_{DS}=30$ V, such as μ_{sat} of 9.7 cm²/V.s, a V_{th} of 5.3 V, SS of 0.77 V/decade, and an I_{ON}/I_{OFF} ratio of 2.5×10^7 . In addition, the forward and reverse sweeps of the TFTs hysteresis are negligible. Figure 4(b and c) transfer and ($I_{DS}-V_{DS}$) shows the output characteristics obtained from the 3% O₂/Ar ratio of a-BIZO TFT. The drain current I_D in the outer curve increased linearly at low-drain-source voltage (V_{DS}), indicating that Ohmic contact was consistently made between the a-BIZO and Mo electrodes and showed clear saturation behavior at high V_{DS} . In addition, no signs were observed of the current crowding phenomenon in the low-drain voltage regime.³⁸

4. CONCLUSION

In summary, we investigated the a-BIZO thin-film as an active channel layer material for oxide TFT fabrication. The a-BIZO thin-films with various O₂/Ar ratios were deposited using sputtering. The structural properties of a-BIZO thin-film were analyzed using XRD and TEM. The amorphous nature of a-BIZO thin-film was confirmed by XRD and TEM. The average transmittance of a-BIZO thin-film was shown to be over 80% in the wavelength ranging between 400 and 800 nm. The 3% O₂/Ar a-BIZO TFT exhibited a saturation field effect mobility of 9.7cm²/V.s, subthreshold swing of 0.77 V/dec, and an I_{ON}/I_{OFF} ratio of 2.5×10^7 . However, the same deposition condition of undoped a-IZO TFT showed a conductive nature. These results indicated that the B₂O₃ dopant strongly suppressed the carrier concentration. The high performance of a-BIZO TFT could be a reason B acts as a strong carrier suppressor, due to the high boron-oxygen bond-dissociation energy and the high Lewis acid strength of B ions. The

high mobility amorphous oxide TFT can be achieved by varying the B doping percentage and various deposition conditions. The results of the present study aid in the design of high performance novel amorphous oxide TFT fabrication.

Acknowledgements

This research was supported by the Basic Science Research Program through the National Research Foundation of Korea (NRF), funded by the Ministry of Science, ICT & Future Planning NRF-2013R1A1A1061213.

REFERENCES

1. K. Nomura, H. Ohta, A. Takagi, T. Kamiya, M. Hirano and H. Hosono, *Nature*, 2004, **432**, 488.
2. T. Kamiya, K. Nomura and H. Hosono, *Sci. Technol. Adv. Mater.*, 2010, **11**, 044305.
3. T. Kamiya, K. Nomura and H. Hosono, *Journal of display Technology*, 2009, **5**, 468.
4. E. Fortunato, L. Pereira, P. Barquinha, A. M. Botelho do Rego, G. Gonçalves, A. Vilà, J. R. Morante and R. F. Martins, *Appl. Phys. Lett.*, 2008, **92**, 222103.
5. M.G. Kim, M. G. Kanatzidis, A. Facchetti and T. J. Marks, *Nature materials*, 2011, **10**, 382.
6. K. Banger, Y. Yamashita, K. Mori, R. Peterson, T. Leedham, J. Rickard and H. Sirringhaus, *Nature materials*, 2010, **10**, 45.
7. T. Arai, *Journal of the Society for Information Display*, 2012, **20**, 156.
8. R. Hayashi, A. Sato, M. Ofuji, K. Abe, H. Yabuta, M. Sano, H. Kumomi, K. Nomura, T. Kamiya and M. Hirano, in *SID Symposium Digest of Technical Papers*, Wiley Online Library, 2008, pp. 621.
9. T. Arai, N. Morosawa, K. Tokunaga, Y. Terai, E. Fukumoto, T. Fujimori, T. Nakayama, T. Yamaguchi and T. Sasaoka, *SID Symposium Digest of Technical Papers*, 2010, **41**, 1033.
10. J. W. Hennek, J. Smith, A. Yan, M.-G. Kim, W. Zhao, V. P. Dravid, A. Facchetti and T. J. Marks, *J. Am. Chem. Soc.*, 2013, **135**, 10729.
11. S. Aikawa, T. Nabatame and K. Tsukagoshi, *Applied Physics Letters*, 2013, **103**, 172105.
12. K. Chang-Jung, K. Sangwook, L. Je-Hun, J.-S. Park, K. Sunil, P. Jaechul, L. Eunha, J. Lee, P. Youngsoo, K. Joo-Han, S. T. Shin and U. i. Chung, *Applied Physics Letters*, 2009, **95**, 252103.
13. E. Chong, Y. S. Chun and S. Y. Lee, *Applied Physics Letters*, 2010, **97**, 102102.

14. J. S. Park, K. Kim, Y. G. Park, Y. G. Mo, H. D. Kim and J. K. Jeong, *Adv.Mater.*, 2009, **21**, 329.
15. H. Kumomi, S. Yaginuma, H. Omura, A. Goyal, A. Sato, M. Watanabe, M. Shimada, N. Kaji, K. Takahashi and M. Ofuji, *Journal of Display Technology*, 2009, **5**, 531.
16. J. C. Park, S. W. Kim, C. J. Kim and H.-N. Lee, *Electron Device Letters, IEEE*, 2012, **33**, 685.
17. J. C. Park, S. W. Kim, C. J. Kim and H.-N. Lee, *Electron Device Letters, IEEE*, 2012, **33**, 809.
18. A. Byung Du, R. You Seung, K. Hyun Jae, L. Jun Hyung, C. Kwun-Bum and P. Jin-Seong, *Journal of Physics D: Applied Physics*, 2014, **47**, 105104.
19. G. H. Kim, W. H. Jeong, B. Du Ahn, H. S. Shin, H. J. Kim, H. J. Kim, M.-K. Ryu, K.-B. Park, J.-B. Seon and S.-Y. Lee, *Applied Physics Letters*, 2010, **96**, 163506.
20. S. Parthiban, J. Y. Kwon, *Journal of Materials Research*, 2014, **29**, 1585.
21. S. Parthiban, S. H. Park, J. Y. Kwon, *Electron Device Letters, IEEE*, 2014, **35**, 1028.
22. J. Kerr, *CRC Handbook of Chemistry and Physics, 81st ed.*, CRC Press, Boca Raton, FL, USA, 2000.
23. S. Calnan and A. Tiwari, *Thin Solid Films*, 2010, **518**, 1839.
24. G. Campet, S. D. Han, S. J. Wen, J. P. Manaud, J. Portier, Y. Xu and J. Salardenne, *Mat. Sci. and Eng. B.*, 1993, **19**, 285.
25. J. G. Lu, Z. Z. Ye, Y. J. Zeng, L. P. Zhu, L. Wang, J. Yuan, B. H. Zhao and Q. L. Liang, *Journal of Applied Physics*, 2006, **100**, 073714.
26. M. F. A. M. van Hest, M. S. Dabney, J. D. Perkins, D. S. Ginley and M. P. Taylor, *Applied Physics Letters*, 2005, **87**, 032111.
27. Y. Zhang, *Inorganic chemistry*, 1982, **21**, 3886.
28. E. Chong, S. H. Kim and S. Y. Lee, *Applied Physics Letters*, 2010, **97**, 252112.
29. N. Mitoma, S. Aikawa, X. Gao, T. Kizu, M. Shimizu, M.-F. Lin, T. Nabatame and K. Tsukagoshi, *Applied Physics Letters*, 2014, **104**, 102103.
30. T. Kizu, S. Aikawa, N. Mitoma, M. Shimizu, X. Gao, M.-F. Lin, T. Nabatame and K. Tsukagoshi, *Applied Physics Letters*, 2014, **104**, 152103.
31. H.-H. Hsieh and C.-C. Wu, *Applied Physics Letters*, 2007, **91**, 013502.
32. M. Bender, N. Katsarakis, E. Gagaoudakis, E. Hourdakis, E. Douloufakis, V. Cimalla and G. Kiriakidis, *Journal of Applied Physics*, 2001, **90**, 5382.
33. B. Kumar, H. Gong and R. Akkipeddi, *Journal of Applied Physics*, 2005, **97**, 063706.
34. I. Hamberg and C. G. Granqvist, *Journal of Applied Physics*, 1986, **60**, R123.
35. E. Burstein, *Physical Review*, 1954, **93**, 632.
36. K. Okamura, D. Nikolova, N. Mechau and H. Hahn, *Applied Physics Letters*, 2009, **94**, 183503.
37. H. Q. Chiang, B. R. McFarlane, D. Hong, R. E. Presley, and J. F. Wager, *J. Non-Cryst. Solids*, 2008, **354**, 2826.
38. T. Kazushige, N. Mitsuru, E. Toshimasa, Y. Hirota and K. Setsuo, *Japanese Journal of Applied Physics*, 2009, **48**, 081606.

Figure 1

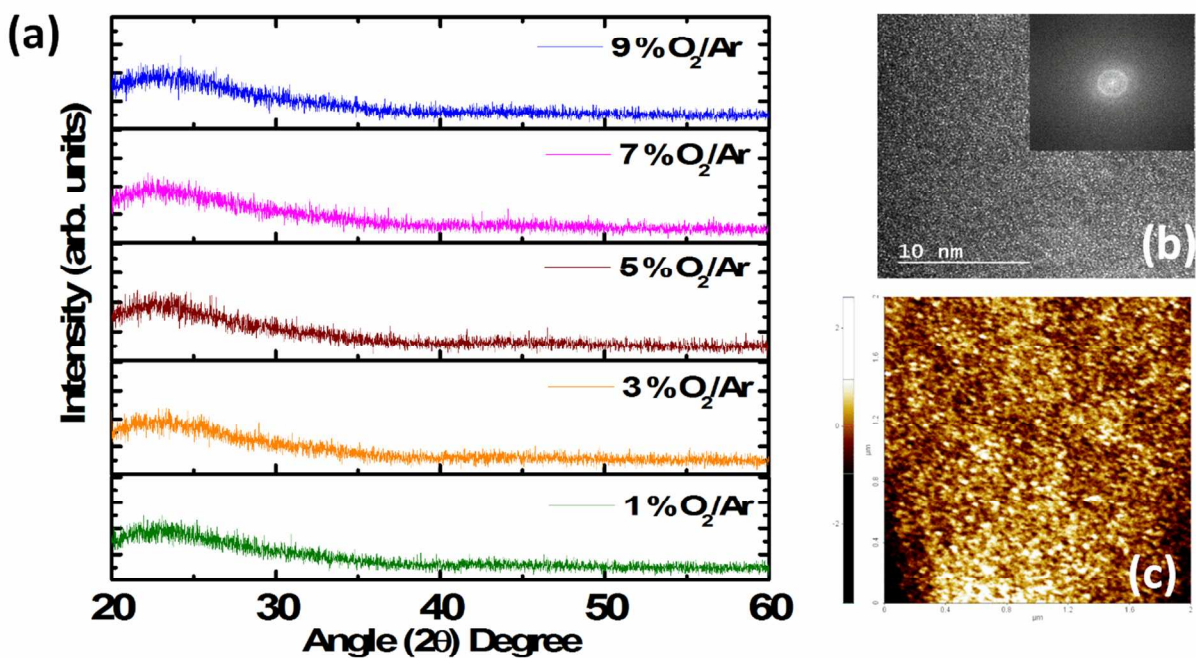


Figure 1. (a) HRXRD patterns of 100 nm thick a-BIZO thin-film coated on Corning glass substrates, (b) HR-TEM image of 3% O₂/Ar a-BIZO thin-film, (c) atomic force microscopy surface of 3% O₂/Ar a-BIZO thin-film

Figure 2

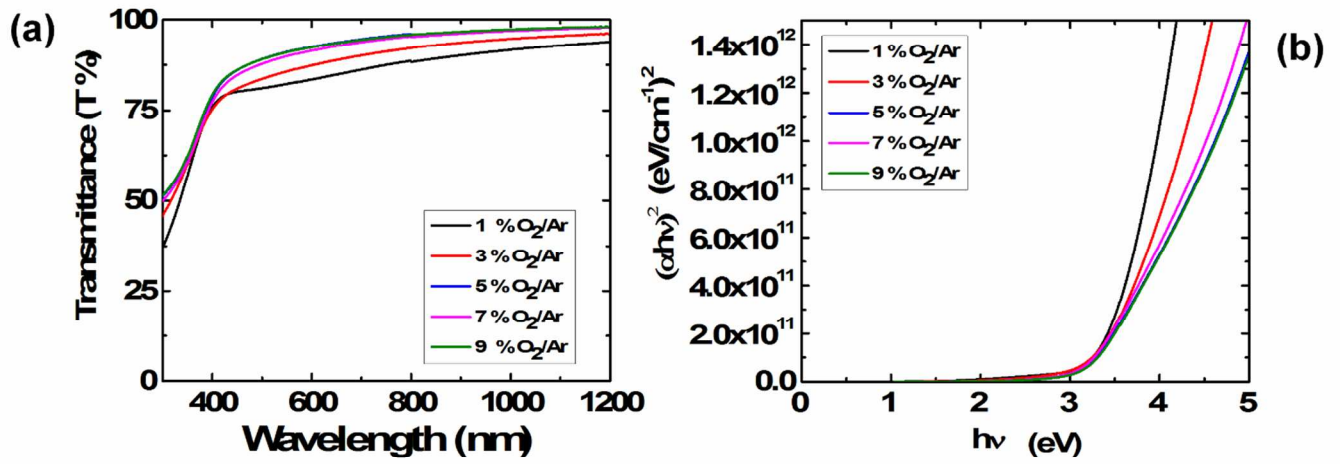


Figure 2. (a) Transmittance spectra, (b) band gap of a-BIZO thin-films with respect to various O₂/Ar.

Figure 3

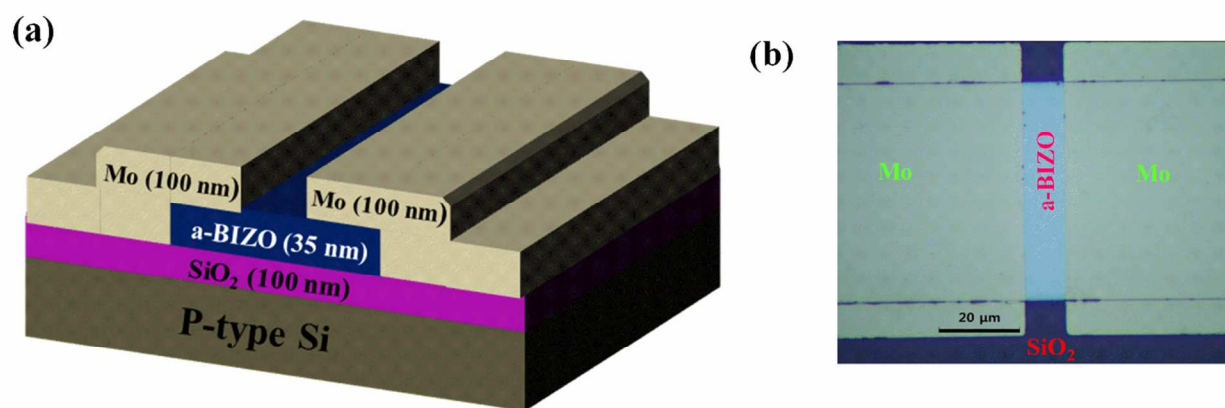


Figure. 3 (a) Schematic diagram of device structure, (b) Optical microscopy top-view image of a-BIZO TFT.

Figure 4

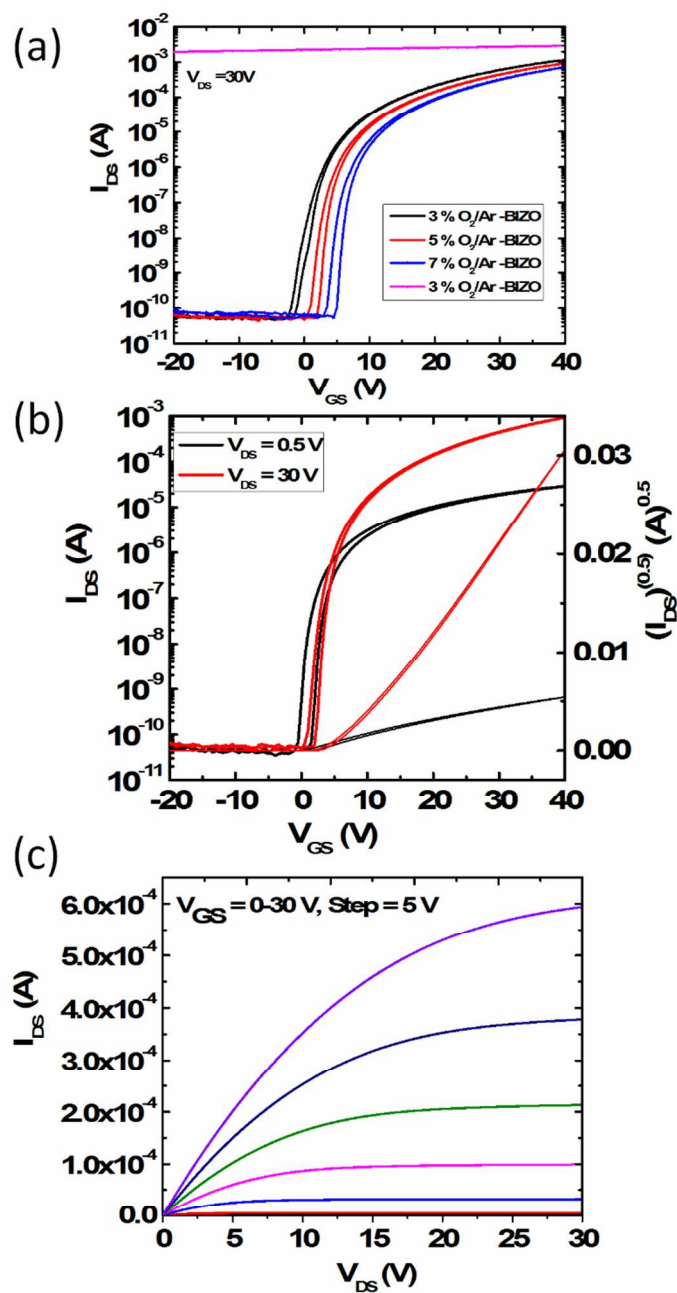


Figure 4.(a) Transfer characteristics of a-IZO and BIZO TFT, (b) and(c) Transfer and output characteristics of 3% Ar/O₂ a-BIZO TFT.

Table.1

Table 1. Bonding dissociation energy and Lewis acid strength of elements.

Elements	Lewis acid strength	Metal-oxygen bond dissociation energy (kJ/mol)
La ³⁺	0.852	799
Ga ³⁺	1.167	353
Hf ⁴⁺	1.462	801
Ta ⁵⁺	1.734	799
Zr ⁴⁺	2.043	776
Ti ⁴⁺	3.064	672
W ⁶⁺	3.158	672
Si ⁴⁺	8.096	799
B ³⁺	10.709	808

Table 2

Table 2. TFT properties of a-BIZO devices.

O ₂ /Ar %	V_{th}	I_{ON}/I_{OFF}	μ_{sat}	SS
	(V)		(cm ² /V.s)	(V/dec)
1	N/A	Conductive	N/A	N/A
3	5.3	2.5×10^7	9.6	0.77
5	7.5	2.2×10^7	8.6	0.60
7	9.9	1.4×10^7	7.7	0.55
9	6.8	3.5×10^5	4.6	0.78